Instability Mode Recognition of Grid-Tied Voltage Source Converters with Nonstationary Signal Analysis

Yu Zhang[1], Sjur Føyen[2], Chen Zhang[1], Marta Molinas[3], Olav Bjarte Fosso[2], Xu Cai[1*]
1 Key Laboratory of Control of Power Transmission and Conversion, SJTU, Shanghai, China
2 Department of Electric Power Engineering, NTNU, Trondheim, Norway
3 Department of Engineering Cybernetics, NTNU, Trondheim, Norway
*E-mail: xucai@sjtu.edu.cn

***Abstract*- With the increasing penetration of voltage-source-converter (VSC) -interfaced distributed generations (DGs) in power systems, oscillation issues have been widely concerned whereas the root cause and nature of the oscillation is sometimes not clear in real cases. This paper focuses on the instability mode recognition (IMR) based on a complete data-driven approach applied to the oscillation waves which can be obtained from the on-site recordings. To this end, we explore the Hilbert-Huang Transform (HHT) for diagnosing the root cause of instability, using only raw data such as the current and voltage waveforms which are accessible by operators. Special attention is paid to distinguish between the sub-synchronous oscillation (SSO) and the loss of synchronization (LOS) as they are two primary instability forms of grid-tied VSC which manifest with very similar waveforms. The pros and cons of the considered signal analysis tools in SSO and LOS recognition are discussed and new lines of investigations are proposed. The analysis and results presented in this paper could shed light on future data-driven analysis, e.g., serving as model-free or hybrid model database for artificial intelligence-based stability diagnosis and recognition.**

Index terms: **signal analysis, converter, oscillation, stability, mode recognition, synchronization, HHT, EMD.**

I. INTRODUCTION

Nowadays, while the power grid is taking the benefit of voltage source converters (VSCs) to enable the integration of various distributed generations (DGs), it also suffers from harmonic oscillation issues caused by power electronic devices, most of which are due to the control interaction against the grid. In this context, two kinds of instability issues of grid-tied VSCs have been frequently reported in practical systems, i.e., the sub-synchronous oscillation (SSO) and the loss of synchronization (LOS) [1]. Both the SSO and LOS are common oscillations in the 0~100Hz frequency range and their oscillation waveforms appear very similar at visual inspection and FFT spectral analysis.

A. Motivation

In the past years, extensive works have been conducted to resolve the oscillation issues of the grid-tied VSCs, especially those relating to stability. Although analytical approaches provide the necessary understanding and insight into these new forms of stability issues, they are merely applicable to simple systems. For practical and complex power systems, modeling the entire system in detail is often restricted by intellectual property issues when different vendors are involved. Besides, prevailing methods based on linear analysis are not sufficient and often fail to reveal the real *essence of harmonics* observed in Fourier spectra, because in such models, no physical source is represented to which harmonics like those coming from PWM, can be attributed. Therefore, the current model-based methods have limited abilities to distinguish among different modes of instability with similar manifestations. For example, if we want to know the reason for the emergence of oscillation near the DG plants, one usual way is to model the whole system and try to reproduce the phenomenon. However, this approach not only implies a huge modelling effort but may also fail to evoke the same instability scenario.

To complement the modelling approach and provide insight from the real system, data-driven approaches can be opted in such cases, and the main advantage is the straightforward use of the on-site signals which carry detail information of the oscillation. To this end, a preliminary step is to identify the instability kind, referred to as *instability mode recognition* (IMR). The restriction of IMR analysis for power system operators is that, in most cases, only the interfacing electrical data (e.g., voltage, current and power) is available for analysis. The lack of internal data of VSC control poses a great challenge to the IMR, which means the IMR should be based on limited accessible signals, such as voltage and currents.

B. Nonstationary Signal Analysis

Frequency is an elemental descriptor of an oscillation, and one might expect different instability modes to show distinct frequency characteristics, yet the ordinary Fourier spectra may be not enough in this context. To be specific, frequency modulation (FM) effect has been reported in both control-involved waveform distortion [2, 3] and harmonic oscillation [4], indicating that the instantaneous frequency (IF) [5, 6] of VSC is constantly varying, rather than discrete frequency components, as is commonly recognized. Besides, the site signals can be rather complex that both the amplitude and the frequency are vary-

This work was supported by the National Natural Science Foundation of China, under Grant 5183700.

ing with time. However, the FFT lacks the ability to analyze such nonstationary signals, and therefore might not be suitable for IMR.

In this regard, nonstationary signal processing methods such as time-frequency analysis (TFA) emerge as promising candidates to explore. There are basically two mainstreams of TFA, according to the definitions of IF. The first is based on the orthogonality of the signal with certain set of bases, e.g., short-time Fourier transform (STFT), Gabor transform, wavelet transforms, which also have the same and intrinsic problem of the *uncertainty principle* as the FT, so that the frequency resolution will lessen if a higher time resolution is obtained by a thinner time window [7]. The second frequency definition is based on the phase time derivative of the complex signal (Section III.A) which is inherently capable to indicate the varying frequency and amplitude of nonstationary signals. However, the definition itself is derived from mono-component signals, and is not suitable for signal containing more than one component.

One prominent solution is the Hilbert-Huang transform (HHT) [8]. The key point is to use the empirical mode decomposition (EMD) technique to sift intrinsic mode functions (IMFs) from the signal, which generally represent components with distinct physical meanings. After the decomposition process, Hilbert transform (HT) is applied on each IMF to process the complex signal, from which the IF and instantaneous amplitude can be calculated. Nevertheless, the strength of EMD is restricted when two signals of close frequency and amplitude are mixed together, resulting in the well-known *mode mixing issue* [9], which has been thoroughly addressed but was not yet solved. Further effort including the ensemble EMD (EEMD) [10], masking signal [11, 12] and heterodyning [13] were reported to mitigate the mode mixing issue, yet there are still some restrictions when using these extended techniques. Moreover, a new method called Fourier decomposition method (FDM) is proposed in [7], which is a promising way to decompose the narrow-band signals and can be a good alternative to EMD. In addition, to improve the computing stability and performance of HT, direct quadrature (DQ) and normalized Hilbert transform (NHT) are proposed in [14] to give a better estimation of the instantaneous frequency.

C. Aim of This Paper

The IMR is urgently called for monitoring and fault analysis of the high-penetrated DG integration, and HHT has shown its great potential to extract the IF from the field signals. To the best of authors' knowledge, IMR has been rarely reported in power system utilities, yet there has not been any attempt on utilizing data-driven-based approaches for this purpose. This paper aims to make an initial exploration that can further indicate its potential usefulness. To motivate a measurement-based analysis of the instability phenomena, we firstly derive the expression of the oscillation signals for SSO and LOS, and present a simple FFT-based spectra. Then, HHT-based method is applied to the same signals, and naturally provides an entirely different inherently nonlinear and non-stationary perspective. We follow up with discussion on the obstacles which must be overcome to pave way for real time IMR.

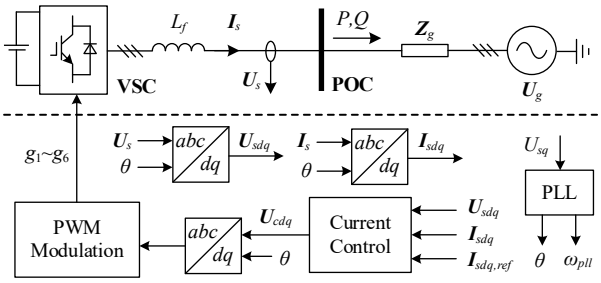

Fig. 1 Schematic diagram of a grid-tied VSC.

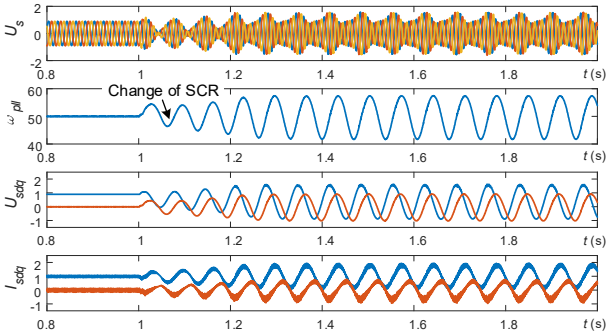

(a) Voltage and frequency waveform profiles for the SSO case

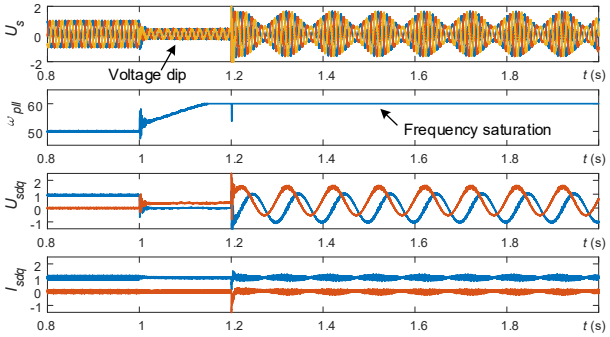

(b) Voltage and frequency waveform profiles for the LOS case

Fig. 2 POC Voltage and PLL frequency profiles of the SSO and LOS. Beat wave effect can be clearly seen for both cases. U_s is three-phase POC voltage, ω_{pll} is PLL frequency, U_{sdq} and I_{sdq} are dq axis voltage and current. Each of the signals are scaled to per unit values.

II. Modelling of Oscillation Waveforms

Although the mechanism of the SSO and LOS has been well understood, currently the analytical expressions of the instability signals are not yet derived. Therefore, we try to recreate the instability signals first, according to the mechanisms described below.

A. Mechanism of The SSO and LOS

The schematic diagram of the grid-tied VSC is shown in Fig. 1. SSO is basically caused by insufficient damping due to strong control interaction against the grid, especially for low SCR systems, which, therefore, can be triggered by both loss of transmission line or mild change of system condition. It is a small-signal instability issue

that occurs in a slowly varying steady-state operating point. When SSO happens, any involving states would oscillate around their equilibrium point, including dq axis voltage U_{sdq}, current I_{sdq} and the frequency of PLL ω_{pll}, as is shown in Fig. 2(a). Therefore, the output voltage is both frequency and amplitude modulated (AM-FM) due to the varying PLL frequency, which agrees with the findings in [4]. Beat wave effect can be observed in the voltage signal at point of connection (POC).

On the other hand, LOS is definitely one kind of large-signal instability caused by severe voltage dip, e.g., short circuit. The basic reason for the LOS is that the PLL frequency diverges upwards during the transient and fail to get back even after the restoring of grid voltage [15], as is shown in Fig. 2(b). Once the LOS occurs, the reference frame of VSC control will never be aligned with the voltage vector at POC, instead, it rotates with a frequency slip and begins to swing. However, the current control still keeps stable and track its reference well, because the instability only involves the PLL. If the converter does not suffer overmodulation, the current could be near perfectly controlled on the dq axis, which is well illustrated in Fig. 2(b). Although there is no AM-FM modulation with LOS signal, the voltage at POC contains at least two components at different frequencies, and the beat waves effect is also observed in the POC voltage signals. Beat waves are also evident in the dq currents.

B. Modelling of The Oscillation Signals

According to the waveforms in Fig. 2(a), assume all signals in dq frame comprise a DC component and a sinusoidal component for the SSO case. Then, the reference voltage is represented by:

$$\begin{cases} U_{sd}(t) = \bar{U}_{sd} + \beta_1 \cos(\omega_h t + \varphi_1) \\ U_{sq}(t) = \bar{U}_{sq} + \beta_2 \sin(\omega_h t + \varphi_1) \end{cases} \tag{1}$$

and the PLL frequency is modelled by:

$$\omega_{pll}(t) = \omega_s[1 + \beta_3 \cos(\omega_h t + \varphi_2)] \tag{2}$$

where $\beta_1, \beta_2, \beta_3$ denote the oscillation amplitude, ω_h the harmonic frequency on the dq axis, φ_1, φ_2 the phase angle, $\bar{U}_{sd}$ and $\bar{U}_{sq}$ the DC component of the voltage, and ω_s the synchronous frequency. The phasor form of (8) is:

$$\mathbf{U}_s^{(dq)}(t) = \bar{U}_c e^{j\varphi_3} + A_1 e^{j(\omega_h t + \varphi_1)} + A_2 e^{-j(\omega_h t + \varphi_1)} \tag{3}$$

where $A_1 = \frac{\beta_1 + \beta_2}{2}$ and $A_2 = \frac{\beta_1 - \beta_2}{2}$. Next, the PLL angle is added to (3) to get the voltage phasor on $\alpha\beta$ axis:

$$\begin{aligned} \mathbf{U}_s^{(\alpha\beta)}(t) &= \mathbf{U}_s^{(dq)}(t) e^{\theta_{pll}(t)} \\ &= \bar{U}_s e^{j(\theta_{pll}(t) + \varphi_3)} + A_1 e^{j(\theta_{pll}(t) + \omega_h t + \varphi_1)} \\ &\quad + A_2 e^{j(\theta_{pll}(t) - \omega_h t - \varphi_1)} \end{aligned} \tag{4}$$

where:

$$\bar{U}_s = \sqrt{\bar{U}_{sd}^2 + \bar{U}_{sq}^2}, \qquad \varphi_3 = \arctan(\bar{U}_{sq}/\bar{U}_{sd})$$

$$\theta_{pll}(t) = \int \omega_{pll}(t) \mathrm{d}t = \omega_s t + \frac{\omega_s}{\omega_h} \beta_3 \sin(\omega_h t + \varphi_2)$$

Equation (4) indicates that the PCC voltage consists of three frequency-modulated signals, as is shown in Table I. The center frequencies of these FM signals are $\omega_s, (\omega_s + \omega_h), (\omega_s - \omega_h)$, that is one center fundamental frequency and two harmonic frequencies in each side. Besides, the *mirror frequency effect*, firstly reported in [16], is also reflected in this modelling while the amplitude of mirror frequency component vanishes when dq axes are symmetric, i.e., $\beta_1 = \beta_2$ or $\beta_1 = -\beta_2$, which also agrees with the findings in [16]. Besides, it should be noted that the frequency of each component of the VSC is oscillating, which is beyond the describing capability of the ordinary linear modelling, for it is only applicable when the frequency oscillation is minor, i.e., $\beta_3 \approx 0$. In short, the waveform of PCC voltage during the SSO includes three AM-FM components of which the IFs are varying around different center frequencies.

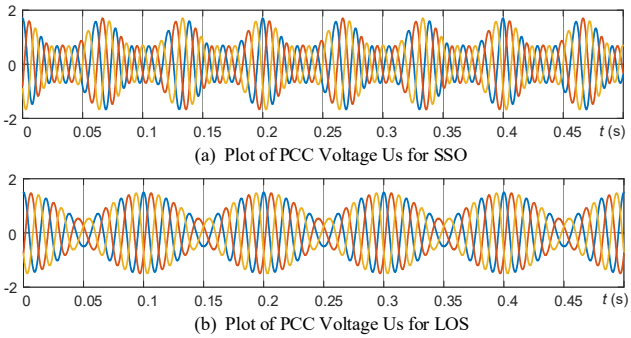

(a) Plot of PCC Voltage Us for SSO

(b) Plot of PCC Voltage Us for LOS

Fig. 3 Recreated artificial signals of instability of the PCC voltage based on assumed modelling in equations (4) and(5).

TABLE I
COMPONENTS IN POC VOLTAGE WHEN SSO OCCURS

Amplitude	Instantaneous Frequency
$\bar{U}_s$	$\omega_s(1 + \beta_3 \cos(\omega_h t + \varphi_2))$
$\frac{\beta_1+\beta_2}{2}\bar{U}_s$	$\omega_s(1 + \beta_3 \cos(\omega_h t + \varphi_2)) + \omega_h$
$\frac{\beta_1-\beta_2}{2}\bar{U}_s$	$\omega_s(1 + \beta_3 \cos(\omega_h t + \varphi_2)) - \omega_h$

For the LOS, assume that the current could always be controlled and is equal to its reference. Then, the PCC voltage is formulated by:

$$\mathbf{U}_s^{(\alpha\beta)}(t) = \bar{U}_g e^{j\omega_s t} + I_s Z_g e^{j(\theta_{pll}(t) + \varphi_4)} \tag{5}$$

where $\boldsymbol{U}_g^{(\alpha\beta)}(t) = \bar{U}_g e^{j\omega_s t}$ denotes the grid voltage vector, $\theta_{pll}(t) = \int \omega_{\mathrm{pll}}(t) \mathrm{d}t$ is the PLL frequency, and φ_4 is the summation of current phase and impedance angle. This indicates, theoretically, that the LOS waveform only contains the background grid voltage and one single FM signal with IF of $\omega_{\mathrm{pll}}(t)$.

According to the voltage expression in (4) and (5), the PCC voltage could reflect the frequency information of the oscillation in VSC, which is crucial to determine which kind of instability is dominant To verify the signal modeling, we use the following values to recreate the signals, and the transient period is temporarily ignored for the sake of simplicity:

$$\bar{U}_{sd} = 0.5, \bar{U}_{cq} = 0.0, \bar{U}_g = 1.0, I_s Z_g = 0.5,$$
$$\beta_1 = 1.2, \beta_2 = 0.8, \beta_3 = 0.15, \varphi_1, \varphi_2 = 0, \varphi_4 = -\tfrac{\pi}{2}$$
for SSO: $\omega_s = 2\pi \times 50\mathrm{Hz}, \omega_h = 2\pi \times 15\mathrm{Hz}$
for LOS: $\omega_{pll}(t) = 2\pi \times 60\mathrm{Hz}$

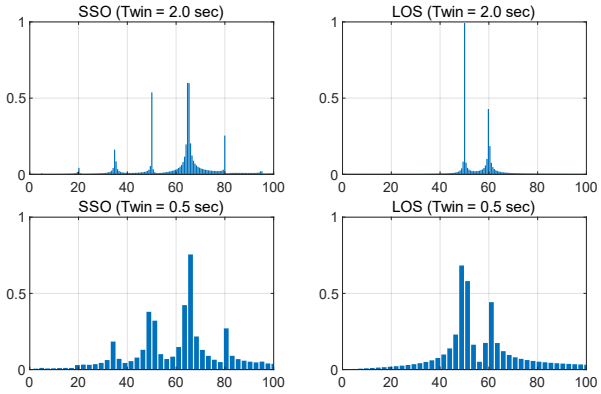

Fig. 4 FFT spectrum of PCC voltage with different time windows. Top and bottom subplots are FFT spectra with time windows of 2s and 0.5s.

The recreated signals are plotted in Fig. 3. These artificial signals resemble the voltage signals in Fig. 2, and the beat wave effect is observed for both SSO and LOS. We remark that (4)~(5) is only one possible modelling.

C. Fourier Analysis on Steady Oscillations

The frequency-domain spectrum with the steady state is investigated via Fast Fourier Transformation (FFT). The FFT spectra are plotted in Fig. 4.

Firstly, we applied FFT on both SSO and LOS at time period of two seconds, and plot the result on the top figures, where the frequency resolution is good. Two main sidebands can be observed in SSO, mostly due to the AM effect (beat wave effect) of the signal, and even more tiny sidebands at $\omega_s \pm k\omega_h$ are distinguishable, which is actually the spectra of FM effect. While for the LOS, there are only two main components in the signal, which is the 50Hz background grid voltage and VSC output voltage at the saturated PLL frequency of 60Hz.

Next, if we reduce the time window to 0.5s, as is shown in the bottom subfigures of Fig. 4., then the frequency resolution is reduced so that the Fourier spectra is blurred, due to the well-known uncertainty principle. For FFT with sampling frequency f_s and N samples, the frequency resolution and required time window are:

$$\Delta f = f_s/N \Rightarrow t_{\text{win}} = N/f_s = 1/\Delta f \tag{6}$$

It implies that if we want to get a better resolution of the frequency, the time window should be extended to several seconds. Therefore, Fourier analysis is applicable at the steady stage of oscillation.

III. Instability Mode Recognition on Transient

In real systems, the signals can be nonstationary, especially for the LOS, which is beyond the capability of FFT analysis. Any other Fourier or wavelet based short-time transform also need enough steady periods for the good performance of TFA. In the following sections, we begin to explore the capabilities of HHT, which has the inherent ability to process nonstationary signals, to give new indicators and criterions for the IMR.

A. The Hilbert-Huang Transform

Suppose $x(t) = a(t)\cos\varphi(t)$ be a mono-component signal with varying amplitude and frequency, where $a(t)$ is the instantaneous amplitude (IA) and $\varphi(t)$ be the phase angle. To obtain the phase angle, the quadrature signal is required, i.e., $y(t) = a(t)\sin\varphi(t)$, which can be obtained from the Hilbert transform (HT):

$$y(t) = \frac{1}{\pi}\int_{-\infty}^{\infty}\frac{x(\tau)}{t-\tau}d\tau \tag{7}$$

Then, complex signal $z(t) = x(t) + jy(t) = a(t)e^{j\varphi(t)}$ is built from the signal $x(t)$ and its quadrature $y(t)$, where the phase angle can be calculated by:

$$\varphi(t) = \arctan(y(t)/x(t)), \tag{8}$$

Then, the IF is defined by:

$$\omega(t) = \frac{\mathrm{d}\varphi(t)}{\mathrm{d}t}. \tag{9}$$

This definition is elegant and meaningful. However, for the signals from the real world, it can be difficult to directly apply due to the following two reasons. First, most of the signals are multi-component and need separation before calculating the IF with (9). Second, HT has many problems in finite signal processing that sometimes yields a poor estimation of the quadrature, which would cause the incorrect computation of the IF and IA.

To solve the first issue, Huang put forward the EMD to sift IMFs from the signal [8]:

1. Let $k = 1$ and $x(t)$ be the initial residual $r_1(t)$;
2. Find the extrema of $r_k(t)$;
3. Interpolate the maxima (minima) to get the upper (lower) envelope $e_{u,k}(t)$ and $e_{l,k}(t)$;
4. Compute the mean of the envelop and assign it as the new residual: $r_{k+1}(t) = (e_{u,k}(t) + e_{l,k}(t))/2$;
5. Subtract the k-th IMF: $s_k(t) = r_k(t) - r_{k+1}(t)$;
6. Check if the *stop criterion* is meet [8]. If not, then let $k = k + 1$ and loop back to procedure No.2.

Finally, the origin signal is decomposed to a series of IMFs $[s_1(t), \ldots, s_{N-1}(t)]$ and one last residual $r_N(t)$:

$$x(t) = r_N(t) + \sum_{k=1}^{N-1} s_k(t) \tag{10}$$

Each IMF is regarded as a mono-component signal, which is intuitively true. However, mode mixing issue is found in EMD when IFs of two components are close to each other. It is theoretically proved in [9] that, for the following signal:

$$x(t) = a_1\cos(2\pi f_1 t) + a_2\cos(2\pi f_2 t + \varphi)\,, f_2 \le f_1 \tag{11}$$

It is only possible to separate each component easily if $af < 1$ and $f < 0.67$, where $a = a_2/a_1$ and $f = f_2/f_1$. Otherwise, the mode mixing will occur and these two components are unable to be separated by ordinary EMD. For example, if we directly use EMD to decompose the SSO signal, the first IMF will be almost the same as the raw signal, as is shown in Fig. 5, because the IF of the components in SSO (see Table I) are quite close with each other so that to cause the mode mixing. This indicates that the first IMF comprises of more than one component and thus the IF shown as Hilbert spectra is meaningless, as is plotted in Fig. 6, because the definition is

only applicable for mono-component signals. The same thing will happen for the LOS signal as well because the IF of PLL is close to that of the background grid voltage.

B. Signal Heterodyning for Decomposition

To solve the mode mixing issue, the frequency ratio between each IMF should be relatively large. To this end, frequency heterodyning is one possibility to alleviate the mode mixing issue, because the spectra of a signal can be shifted by multiplying a heterodyning signal [13]. Given a two-component real signal:

$$x(t) = A_1(t)\cos 2\pi f_1 t + A_2(t)\cos 2\pi f_2 t \tag{12}$$

Its spectra can be shifted by signal heterodyning:

$$\begin{aligned} x_{hd}(t) &= x(t)\cdot 2\cos 2\pi f_{hd} t \\ &= A_1(t)\cos 2\pi \Delta f_1 t + A_2(t)\cos 2\pi \Delta f_2 t \\ &\quad + A_1(t)\cos(2\pi(f_1+f_{hd})t) \\ &\quad + A_2(t)\cos(2\pi(f_2+f_{hd})t) \end{aligned} \tag{13}$$

where $\Delta f_1 = f_1 - f_{hd}$ and $\Delta f_2 = f_2 - f_{hd}$. Let f_{hd} be slightly lower (or greater) than the smaller (larger) one of $\{f_1, f_2\}$, then it will be possible to find such f_{hd} to meet the requirement of decomposition. Two components of higher frequency are also produced, which is obviously out of the octave of the first two. Therefore, the IMFs for these high-frequency components can be filtered or decomposed easily and should be discarded.

For balanced three-phase systems, the space vector of voltage and current can be obtained by Clarke transform on three-phase signals. Therefore, complex demodulation can be adopted instead of signal heterodyning for better performance, since it can shift the frequency without producing high frequency components. We give an example on how the complex demodulation works. Given a two-component complex signal:

$$z(t) = A_1(t)e^{\mathrm{j}2\pi f_1 t} + A_2(t)e^{\mathrm{j}2\pi f_2 t} \tag{14}$$

Complex rotation $e^{-\mathrm{j}2\pi f_{hd} t}$ is adopted for heterodyning:

$$\begin{aligned} x_{hd}(t) &= \mathrm{Re}\{x(t)\cdot e^{-\mathrm{j}2\pi f_{hd} t}\} \\ &= \mathrm{Re}\{A_1(t)e^{\mathrm{j}2\pi f_1 t} + A_2(t)e^{\mathrm{j}2\pi f_2 t}\} \\ &= A_1(t)\cos 2\pi \Delta f_1 t + A_2(t)\cos 2\pi \Delta f_2 t \end{aligned} \tag{15}$$

The decomposition performance relates much with the heterodyning frequency. For the SSO, because there are three oscillating components at the center frequency of $\omega_s, (\omega_s+\omega_h), (\omega_s-\omega_h)$, and it can be hard to choose a single heterodyning frequency to separate them all. One possible solution is to set $f_{hd} = 50\mathrm{Hz}$, so that the center frequencies of each will be shifted to $0\mathrm{Hz}$ and $\pm\omega_h$, respectively. According to the expressions in Table I, the last two components will mix with each other as one single component with mean frequency of ω_h:

$$\begin{aligned} &\tfrac{\beta_1+\beta_2}{2}\cos\left(\omega_h t + \tilde{\theta}(t)\right) + \tfrac{\beta_1-\beta_2}{2}\cos\left(-\omega_h t + \tilde{\theta}(t)\right) \\ &= \beta_1\cos\tilde{\theta}(t)\cos\omega_h t - \beta_2\sin\tilde{\theta}(t)\sin\omega_h t \\ &\approx \beta_1\cos\omega_h t - \beta_2\tilde{\theta}(t)\sin\omega_h t \\ &= \sqrt{\beta_1^2+\beta_2^2\tilde{\theta}^2(t)}\cos\left(\omega_h t + \tan^{-1}\left(\beta_2\tilde{\theta}(t)/\beta_1\right)\right) \end{aligned} \tag{16}$$

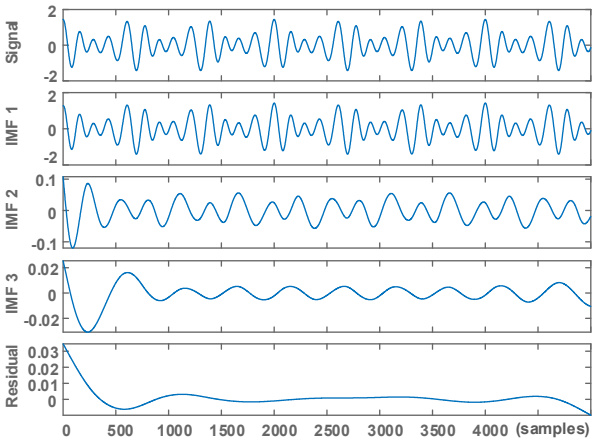

Fig. 5 EMD for the artificial SSO signal U_{sa} where mode mixing occurs.

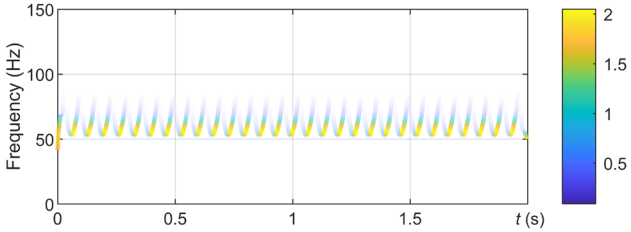

Fig. 6 Hilbert spectra for the first IMF (IMF1 in Fig. 5) of SSO through the ordinary EMD. The colormap denotes the IA of the complex signal.

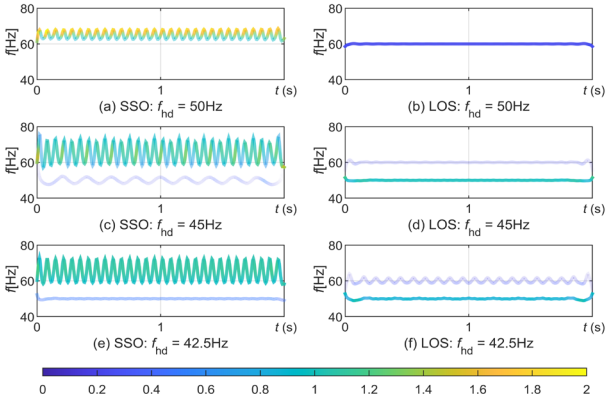

Fig. 7 Hilbert spectra for the IMF of instability mode of SSO (left) and LOS (right) with different heterodyning frequencies.

where $\tilde{\theta}(t)$ denotes the oscillating term in Table I. If $\beta_2 < \beta_1$, then the oscillation of the IF will be lessened, which will be shown later that can pose a threat to the IMR if the indicator becomes less distinct. Therefore, some other frequencies should be tried so as to find the best one.

For illustration, we decomposed the artificial signals by three heterodyning signals at $50\mathrm{Hz}, 45\mathrm{Hz}$ and $42.5\mathrm{Hz}$. The IFs representing the instability mode of the SSO are plotted in Fig. 7(a)(c)(e). It can be seen that the mean of IF is $65\mathrm{Hz}$, and the vibration frequency of the IF is $15\mathrm{Hz}$, which coincides with the analysis above. For the SSO, the IF variation of 65Hz-component with $f_{hd} = 50\mathrm{Hz}$ is lower than that of the others, which verified the analysis above. In comparison, the IFs of the instability mode for LOS case are plotted in Fig. 7(b)(d)(f). A 60-Hz component is observed in the spectra and there is no distinct oscillation on the IF as is found in the SSO case. When $f_{hd} = 42.5\mathrm{Hz}$, the best decomposition performance for

SSO is witnessed, as the $(\omega_s + \omega_h)$ component is isolated from the others; While for the LOS, this heterodyning frequency gives the worst result for the frequency shift is not enough for EMD to work well. It shows that the IF can be a good indicator to distinguish the LOS from SSO.

C. The Proposed Method

1) Algorithm for extracting the instability signal

Now an overview of the whole procedure to separate the instability oscillation signal from either SSO or LOS is described below. Some additional measures are taken to improve the decomposition of the results:

1. Apply Clarke Transform to the three-phase signal, or skip this if a single-phase signal is used;
2. Take signal heterodyning or complex demodulation to shift the spectra (try on different f_{hd} for the good of EMD performance);
3. Pass the signal through a lowpass filter;
4. Decompose with EMD to obtain IMFs;
5. Calculate the IF and IA for each IMF by HT, DQ, NHT or other else methods;
6. Add the heterodyning frequency to each IF, and plot the Hilbert spectrum.

The lowpass filter is used to smooth the transients and remove high frequency dynamics and noises, which is crucial to get good results. This step should be placed after the frequency shifting, which could facilitate the use of filter with lower cut-off frequency. Besides, this process is regarded as one standard preprocess of EMD for the purpose of anti-aliasing, and discrete events so that we can process EMD with a lower sampling frequency.

2) Criteria on instability mode recognition

From the procedure above, the first criterion to judge whether an oscillation within 0~100Hz is SSO or LOS is by observing the IF oscillation:

Criterion I: *In steady oscillating period, if regular oscillation is observed in the target IF, of which the oscillating frequency is the same as the frequency difference between the mean of the target IF and the fundamentals, then the instability mode should be the SSO; otherwise, it should be the LOS.*

Naturally, real measurement devices contain transients as well. The transient also conveys information of the type of instability, due to the frequency evolution process with different kind of instability. As is shown in Fig. 2, the frequency of PLL is not constant during the voltage dip, but keeps climbing until reaching the limitation. Therefore, the transient period will help with the IMR of the VSC, which gives rise to the second criterion:

Criterion II: *If a recognizable rise is observed in the target IF in the transient process, then the instability mode should be the LOS; otherwise, it should be SSO.*

As HHT is intended precisely for extraction of physically relevant information of multicomponent, nonlinear and nonstationary waveforms, there is no need to restrict analysis to the steady state, which means that the proposed method to extract the target IF is also applicable to the transients. We shall show in the following section how the HHT-based IMR algorithm enables joint use of transient and steady-state stages.

IV. Simulation Tests

A. Verification on Simulation Signals

The first case will demonstrate the procedure for both the SSO and LOS. The circuit topology is shown in Fig. 1, and the simulation settings are the same as well to trigger the SSO and LOS, of which the waveforms are shown in Fig. 2. Only the signals of POC can be used for IMR, e.g., voltage and current. A heterodyning frequency of 45Hz is adopted for the LOS and 43Hz for the SSO. Three-phase POC voltage signals are processed in this case, which is: (1) passed through a 3rd-order Butterworth lowpass filter, (2) rotated (heterodyned) with a 45Hz/43 Hz complex exponential, (3) decomposed with EMD. Then, through the direct quadrature [14], the instantaneous frequency is yielded for each IMF. The heterodyning frequency is added to the IF. Finally, the Hilbert spectrum is calculated from the IF and IA, then filtered with a gaussian filter for a smooth appearance.

The resulting spectra are shown in Fig. 8, where the analysis is based on windows from $t = 0.3$s to $t = 2.5$s. The long duration of the signal is needed to ensure that the heterodyned signal has enough periods for EMD to work well. But this is not an insurmountable restriction, for example, joint use of masking signals and heterodyning has potential to reduce the required length of the time window. As can be clearly seen from the first figure, the VSC suffered a period of low voltage before the fault is cleared, during which the IF of one IMF went through an obvious rising, which indicates that the oscillation mode is LOS. While for the other one, a distinct oscillating frequency appears suddenly above the fundamental frequency, hence the oscillation mode is SSO.

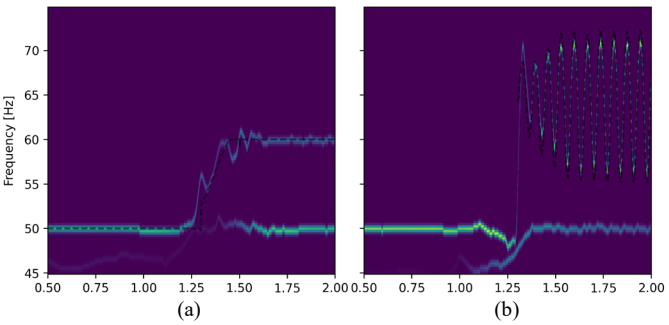

Fig. 8 Hilbert spectra of the voltage measurements after heterodyning and EMD. (a) LOS. Dashed black line is the PLL frequency. (b) SSO. For comparison, the dashed black line is the PLL frequency for the LOS, and the PLL frequency plus the oscillating frequency for the SSO.

B. Measurement quality

At first sight it might be unclear how to select measurements for IMR. Which is the better choice of voltage and current to be a good indicator? Where should the measurements be located? To answer these questions, we discuss a few challenges with the decomposition and some traits of the signals. The current and voltage measurements are decomposed by the aforementioned process and the results are plotted in Fig. 9 and Fig. 10, we will see that the current signal is more distinct as an instability indicator for the LOS case, and decomposition of the

current is not strictly necessary. This is because the converter regulates the current to follow the frequency of the PLL, while it (almost) suppresses the fundamental. The same argument does not hold true for the PCC voltage measurements, as the current at the fundamental is suppressed, the grid PCC voltage must equal the grid voltage. In the SSO case for a single VSC, there is no such clear distinction between the current and voltage measurements, for they will both have a nonnegligible fundamental and hence must be decomposed. The LOS presents the greatest challenge for IMR, due to the short duration of the fault. The amplitude of the LOS and fundamental should be slowly varying or constant in the entire window, lest the frequency information be obscured.

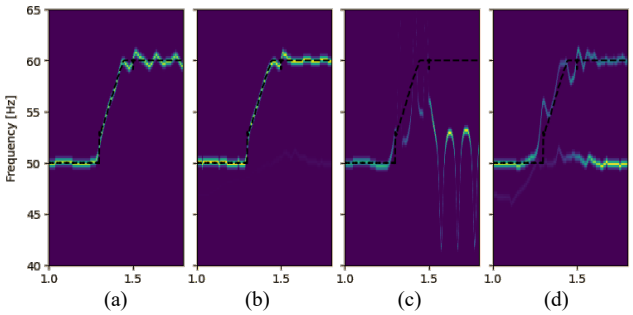

Fig. 9 Hilbert spectra for current and voltage for the LOS case, with or without decomposition. (a) current without EMD, (b) current with EMD, (c) voltage without EMD, (d) voltage with EMD.

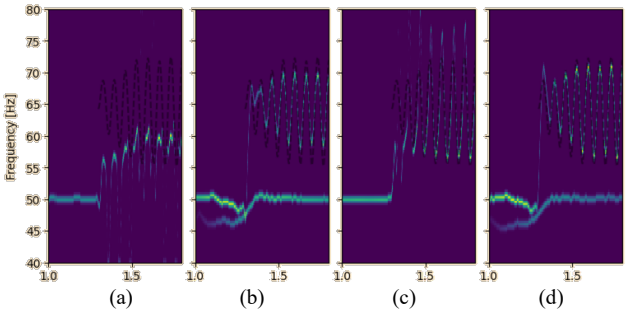

Fig. 10 Hilbert spectra for current and voltage for the SSO case, with or without decomposition. (a) current without EMD, (b) current with EMD, (c) voltage without EMD, (d) voltage with EMD.

The PCC current meets this criterion (no need for decomposition) for the single converter case, but we present a multi-converter system to illustrate that it is not always so. The performance of the proposed decomposition is examined in multi-converter network, as is illustrated in Fig. 11, where two converter stations are connected in parallel to a bus with a local load. The SC fault is applied on the common bus for 200ms to trigger the LOS.

The spectra for the LOS case are shown in Fig. 12. It seems as if the target IMF of the PCC voltage is hardly visible, as its amplitude is very low compared to the fundamental. More importantly, the LOS ramp is not visible. However, if we decompose the PCC current, then we could obtain the spectra in Fig. 13(a), which looks much clearer than the voltage. It seems that the current is a better indicator than the voltage, for it wouldn't attenuate as the distance increases, but the decomposition is needed because the PCC current contains both the LOS signal from the faulted VSC and the normal signal at 50Hz.

Moreover, the LOS IMF can be weakened by the load current, as is shown in Fig. 13(b), which indicates that measuring the current that goes to the grid is not very robust. Therefore, the measurement position is also very crucial to the IMR and need further exploration.

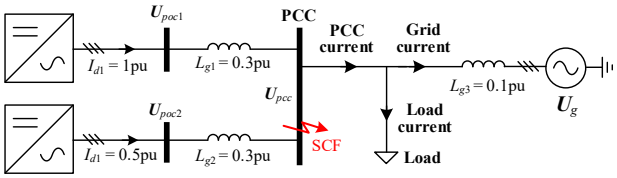

Fig. 11 Test case for multi-converter network scenario.

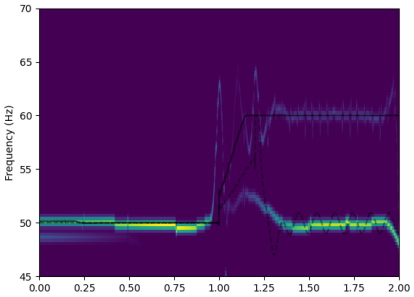

Fig. 12 Hilbert spectrum of the PCC voltage for multi-converter system.

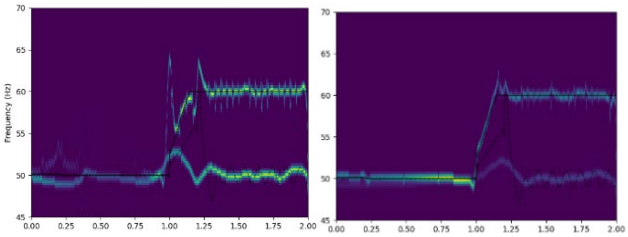

Fig. 13 Hilbert spectrum of the current (a) PCC current which excludes the load current; (b) grid current which includes the load current.

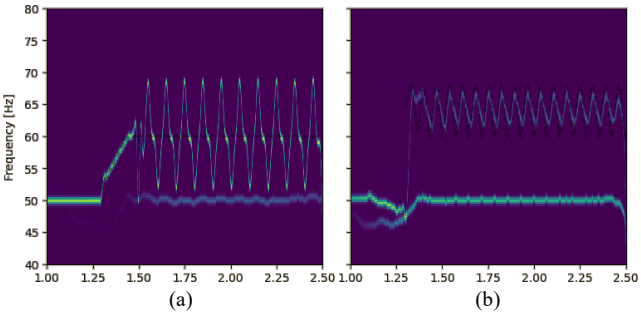

Fig. 14 Hilbert spectra for the decomposed current when overmodulation happens in (a) LOS and (b) SSO.

C. *Overmodulation Effects*

Both LOS and SSO are likely to inflict overmodulation on the converter. Though normally interpreted in terms of the harmonic spectrum, we apply the same procedure to see the instantaneous properties of POC current during overmodulation, the results are shown in Fig. 14.

The same analysis on the POC voltages is omitted, though it yields similar spectra. The LOS ramp is still captured very well, as overmodulation takes effect only after the fault is cleared. However, the LOS IMF exhibits larger frequency oscillations than the SSO in steady state,

which is caused by more severe overmodulation of LOS than of SSO. Therefore, the performance of the proposed method highlights the importance of criterion II. Further investigations are needed to determine if the steady state can be included in IMR, or if overmodulated SSO and LOS IMFs are practically indistinguishable.

V. Conclusion

This paper focuses on the IMR issue of the VSCs via interfacing measurement signals. We concluded that two ordinary kinds of instability within 0~100Hz, namely the SSO and LOS, can be identified and be distinguishable from each other by complete data-driven approach. We firstly recreate the PCC voltage signal for the SSO and the LOS, in order to obtain the key features of the signals from their mathematical expressions. FFT is firstly applied to get the frequency spectrum for the initial cognition of the instability signals. It is found that the frequency component of the converter output voltage and the background grid voltage are so close that the EMD dependent mode mixing issue can possibly happen, which is then verified by applying EMD on the raw signal of PCC voltage. Complex demodulation (signal heterodyning) is adopted to shift the background 50Hz signal to a very low frequency component, so that the instability IMF can be isolated and analyzed. In this way, the residual signal only contains the converter output that reflects the frequency variation in the converter. Two criteria for IMR of SSO and LOS are put forward, where we remark on the importance of transient stage of the signals. Besides, we also discuss on the need for decomposition for voltage and current signals, improve the performance on multi converter system, and make suggestion on the measurement location. Finally, we observed the current signal could be distorted due to overmodulation and thus the corresponding IMF profile will be affected. However, since the signal hasn't been rebuilt to reflect the overmodulation effect, this issue is not well resolved and hence need further investigation.

VI. Acknowledgement

The authors would like to acknowledge the open access publication support to the project "NTNU-Chinese Collaboration on Next Generation Power Electronics Converters for Renewable Energy (CoNeCt)" 309253 funded by the Research Council of Norway under the INTPART programme.

References

[1] J. Shair, H. Li, J. Hu, and X. Xie, "Power system stability issues, classifications and research prospects in the context of high-penetration of renewables and power electronics," *Renewable and Sustainable Energy Reviews,* vol. 145, 2021, doi: 10.1016/j.rser.2021.111111.

[2] G. Kulia, M. Molinas, L. Lundheim, and B. B. Larsen, "Towards a real-time measurement platform for microgrids in isolated communities," *Procedia engineering,* vol. 159, pp. 94-103, 2016.

[3] G. Kulia, M. Molinas, and L. Lundheim, "Tool for detecting waveform distortions in inverter-based microgrids: a validation study," in *2016 IEEE Global Humanitarian Technology Conference (GHTC)*, 2016: IEEE, pp. 525-531.

[4] R. Ma, Z. Yang, S. Cheng, and M. Zhan, "Sustained Oscillations and Bifurcations in Three-phase VSC Tied to AC Gird," *IET Renewable Power Generation,* 2020.

[5] B. Boashash, "Estimating and interpreting the instantaneous frequency of a signal. I. Fundamentals," *Proceedings of the IEEE,* vol. 80, no. 4, pp. 520-538, 1992, doi: 10.1109/5.135376.

[6] B. Boashash, "Estimating and interpreting the instantaneous frequency of a signal. II. Algorithms and applications," *Proceedings of the IEEE,* vol. 80, no. 4, pp. 540-568, 1992, doi: 10.1109/5.135378.

[7] P. Singh, "Breaking the limits: redefining the instantaneous frequency," *Circuits, Systems, and Signal Processing,* vol. 37, no. 8, pp. 3515-3536, 2018.

[8] N. E. Huang *et al.*, "The empirical mode decomposition and the Hilbert spectrum for nonlinear and non-stationary time series analysis," *Proceedings of the Royal Society of London. Series A: mathematical, physical and engineering sciences,* vol. 454, no. 1971, pp. 903-995, 1998.

[9] G. Rilling and P. Flandrin, "One or Two Frequencies? The Empirical Mode Decomposition Answers," *IEEE Transactions on Signal Processing,* vol. 56, no. 1, pp. 85-95, 2008, doi: 10.1109/tsp.2007.906771.

[10] Z. Wu and N. E. Huang, "Ensemble empirical mode decomposition: a noise-assisted data analysis method," *Advances in adaptive data analysis,* vol. 1, no. 01, pp. 1-41, 2009.

[11] O. B. Fosso and M. Molinas, "EMD mode mixing separation of signals with close spectral proximity in smart grids," in *2018 IEEE PES innovative smart grid technologies conference Europe (ISGT-Europe)*, 2018: IEEE, pp. 1-6.

[12] R. Deering and J. F. Kaiser, "The use of a masking signal to improve empirical mode decomposition," in *Proceedings. (ICASSP'05). IEEE International Conference on Acoustics, Speech, and Signal Processing, 2005.*, 2005, vol. 4: IEEE, pp. iv/485-iv/488 Vol. 4.

[13] N. Senroy and S. Suryanarayanan, "Two techniques to enhance empirical mode decomposition for power quality applications," in *2007 IEEE Power Engineering Society General Meeting*, 2007: IEEE, pp. 1-6.

[14] N. E. Huang, Z. Wu, S. R. Long, K. C. Arnold, X. Chen, and K. Blank, "On instantaneous frequency," *Advances in adaptive data analysis,* vol. 1, no. 02, pp. 177-229, 2009.

[15] D. Dong, B. Wen, D. Boroyevich, P. Mattavelli, and Y. Xue, "Analysis of phase-locked loop low-frequency stability in three-phase grid-connected power converters considering impedance interactions," *IEEE Transactions on Industrial Electronics,* vol. 62, no. 1, pp. 310-321, 2015, doi: 10.1109/TIE.2014.2334665.

[16] A. Rygg, M. Molinas, C. Zhang, and X. Cai, "A Modified Sequence-Domain Impedance Definition and Its Equivalence to the dq-Domain Impedance Definition for the Stability Analysis of AC Power Electronic Systems," *IEEE Journal of Emerging and Selected Topics in Power Electronics,* vol. 4, no. 4, pp. 1383-1396, 2016, doi: 10.1109/JESTPE. 2016.2588733.